Journal of
Ceramic Science
and Technology

J. Ceram. Sci. Technol., **14** [1] 39-48 (2023)
DOI: 10.4416/JCST2023-00002
available online at: http://www.ceramic-science.com

Short Communication

Sintering and High-Temperature Strength of (Ti,Hf,Ta)C Medium-Entropy Ceramics Consolidated by Biphasic Carbide Powders

F.L. Qin[1, 2], X.G. Wang[*2], X.F. Wang[2], Q.Q. Yang[2], R.Z. Li[2], W. Gao[2], C. Zhang[*1], D.Y. Jiang[2]

[1]School of Materials Science and Engineering, Shanghai Institute of Technology, Shanghai 201418, China
[2]State Key Laboratory of High Performance Ceramics and Superfine Microstructure, Shanghai Institute of Ceramics, Shanghai 200050, China

received Febuary 15, 2023; received in revised form March 24, 2023; accepted March 27, 2023

Abstract

This study reports for the first time on the preparation of medium-entropy (Ti,Hf,Ta)C-based powders with biphasic composition of Hf(Ti,Ta)C and Ti,Ta(Hf)C based on carbothermal reduction of TiO_2, Ta_2O_5 and HfO_2 with graphite. The synthesized (Ti,Hf,Ta)C-based powders had a fine particle size of 200 – 300 nm and low oxygen content of 0.42 wt%. After sintering at 2 100 °C for 1 h, single-phase (Ti,Hf,Ta)C ceramics were obtained. The effect of the Hf element content on the densification and grain growth of (Ti,Hf,Ta)C medium-entropy ceramics was investigated and compared with monocarbide ceramics (TiC, HfC, TaC). The final sintered medium-entropy (Ti,Hf,Ta)C ceramics prepared by means of hot pressing at 2 100 °C had fine grains (0.92 ± 0.4 µm) and a relative density of 93.3 %. The Hf element significantly inhibited the densification and grain growth of (Ti,Hf,Ta)C ceramics due to its lattice distortion and the sluggish diffusion effects. The equimolar ratio (Ti,Hf,Ta)C corresponding to ($Ti_{1/3}Hf_{1/3}Ta_{1/3}$)C had ultra-high strength at 1 600 °C (639 ± 38 MPa) and 1 800 °C (697 ± 26 MPa). The ultra-high strength of (Ti,Hf,Ta)C medium-entropy ceramics is the result of the collaborative optimization of the superfine microstructure (grain size of 0.92 ± 0.4 µm) and strong grain boundary strength.

Keywords: Medium-entropy ceramics (Ti,Hf,Ta)C, sluggish diffusion effect, high-temperature flexural strength.

I. Introduction

At present, as human beings are becoming more curious about the expansion of unknown areas, demand is growing for materials to meet requirements in extreme service environments. Ultra-high-temperature ceramics (UHTCs) are a limited and select set of carbides, nitrides and borides of the group IV and V transition metals [1–3]. UHTCs have the highest melting points of any known compounds, making them suitable for use in extreme environments [4]. They are characterized by a unique combination of properties, including melting points above 3 500 K, high-temperature strength and the capability to conduct heat when the service temperatures exceed 2 200 K [5]. A variety of UHTC developments have been reported in the past twenty years, highlighting significant advantages for some applications [6–11]. As an example, potential applications for carbide ceramics in the aerospace industry have been considered, such as the sharp leading domes and wing edges of hypersonic flight vehicles [12]. The first results on multicomponent and high-entropy crystal alloys were published in 2004 [3, 13, 14]. This new concept includes the opening up of a vast and unexplored field of alloy composition and the potential to influence the stability of solid-solution phases by controlling configurational entropy. This very different idea has captured the imagination and efforts of a growing number of people in the materials science community. The method of creating the solid solutions was inspired by the development of multi-metal solid-solution compounds. It is a new type of ultra-high-temperature ceramics (UHTCs) developed based on transition metal carbide [7–9, 15] and diboride [6, 16–18]. High-entropy carbide ultra-high-temperature ceramics have attracted more and more attention owing to their excellent properties such as high hardness, high strength and high toughness [6–11].

The synthesis, densification, and microstructure of high-entropy carbides ceramics are the main factors influencing their mechanical properties. High-entropy carbides ceramics powders have been synthesized from commercial carbide powders [19], carbothermal reduction of oxides [8, 9], liquid precursors [20, 21], and the reaction of elemental metals with carbon sources [22]. Demirskyi *et al.* [7] used commercial TaC, TiC, and ZrC as raw materials to prepare single-phase ($Ta_{1/3}Ti_{1/3}Zr_{1/3}$)C ceramics by means of SPS at 1 973 °C. The flexural strength and fracture toughness of ($Ta_{1/3}Ti_{1/3}Zr_{1/3}$)C at room tempera-

* Corresponding author: xgwang@mail.sic.ac.cn
co-corresponding author: czhang@sit.edu.cn

ture reached an average of 700 MPa and 3.2 MPa·$m^{1/2}$, respectively. At 1 600 °C, the flexural strength decreased by 300 ± 25 MPa, and there was no significant change at 1 800 °C. At 1 800 °C, $(Ta_{1/3}Ti_{1/3}Zr_{1/3})C$ ceramics undergo local decomposition, forming a structure with local chemical gradient, and the fracture toughness increases by 30 % (up to 4.4 MPa·$m^{1/2}$). Wang *et al.* [9] prepared an ultrafine-grained (Ti,Zr,Hf)C ceramic by means of carbothermal reduction of oxides, which exhibits extremely high strength at ultrahigh temperature, with a flexural strength of 619 ± 57 MPa at 1 600 °C and no obvious degradation even at 1 800 °C. The main strengthening mechanism in (Ti,Zr,Hf)C can be attributed to the high lattice parameter mismatch effect between TiC and ZrC. Yang *et al.* [8] sintered (Ti,Zr,Ta)C ceramics at 2 100 °C using core-shell powders with low oxygen content. The ultra-high- strength properties of (Ti,Zr,Ta)C ceramics were studied. It was found that their core-shell structure can effectively inhibit the increase of grain size (1.1 ± 0.4 μm), and further improve the high-temperature properties of the materials. The flexural strength of (Ti,Zr,Ta)C at 1 000 °C (493 ± 21 MPa) is close to that at room temperature (511 ± 52 MPa). With temperature increase from 1 600 °C to 1 800 °C, the flexural strength increased significantly, reaching 725 ± 32 MPa at 1 800 °C. Xu *et al.* [17] successfully prepared (Hf,Zr,Ta,Nb,Ti)B_2 ceramics sintered with cobalt as an additive by means of spark plasma sintering at 1 500 °C. The relative density increased from 49.3 % to 99.5 %. The grain size was refined to 0.5 μm. This shows that the use of additives plays an important role in the modification of ceramics. Feng *et al.* [21] used metal oxides and carbon black as original materials to prepare high-entropy (Hf,Zr,Ti,Ta,Nb)C ceramics in a two-step process of carbon-thermal reduction and hot pressing. It was found that the flexural strength of (Hf,Zr,Ti,Ta,Nb)C carbide ceramics decreased above 1 800 °C due to the decrease in dislocation density and increase in dislocation movement. Li *et al.* [22] reported on a simple liquid precursor method for the synthesis of single-phase high-entropy carbide nanopowders. The as-synthesized powders possess an average particle size of 132 ± 5 nm, a specific surface area of 24.5 m^2/g, and an oxygen content of 0.22 wt%, respectively.

Guo *et al.* [23] studied and prepared high-entropy (Ti,Zr,Hf,Nb,Ta)C ceramics, and found that high-entropy ceramics maintained the integrity of crystal structure, and uniform distribution of solid-solution elements at micro scale. Meanwhile, solid-solution elements concentration oscillations, atomic dispersion and lattice strain were observed at the nanoscale.

The microstructural evolution of high-entropy ceramics also has great influence on their mechanical properties. The impurities existing in ceramic grain boundaries and the relatively rough grain boundaries could improve the high-temperature flexural strength of high-entropy carbide. Zhang *et al.*[24] studied the grain growth kinetics and densification mechanism of high-entropy (Ti,Zr,Hf,V,Nb,Ta)C ceramics. Sintering of the ceramics at 2 300 °C will form single-phase carbides with rock salt structure, before which the corresponding V, Zr, Hf will appear [GS1] obvious aggregation phenomenon. With the increase in sintering temperature, the grain growth mechanism gradually changes from surface diffusion to volume diffusion, and then to grain boundary diffusion. The solid solution formation can effectively promote the densification process based on the design of two-step sintering. Liu *et al.* [6] reported the high-temperature strength of $(Ti_{0.2}Zr_{0.2}Nb_{0.2}Hf_{0.2}Ta_{0.2})B_2$ high-entropy diboride ceramics and discussed the high-temperature strengthening mechanism. The high-entropy boride ceramics with ~ 2 vol% oxides and ~ 1 vol% porosity were successfully consolidated by means of spark plasma sintering at 2 000 °C. The flexural strength of $(Ti_{0.2}Zr_{0.2}Nb_{0.2}Hf_{0.2}Ta_{0.2})B_2$ reached 400.4 ± 47.0 MPa at room temperature and 751.6 ± 23.2 MPa at 1 800 °C, respectively. Yang *et al.*[25] also studied the influence of equiatomic Zr/(Ti,Nb) substitution on the high-temperature strength of (Ti,Zr,Nb)C medium-entropy ceramics. The grain size of (Ti,Zr,Nb)C ceramics decreased from 9.4 ± 3.7 μm for $(Ti_{0.45}Zr_{0.1}Nb_{0.45})C$ to 1.1 ± 0.4 μm for $(Ti_{1/3}Zr_{1/3}Nb_{1/3})C$, due to the sluggish diffusion effect of increasing the configuration entropy. At 1 900 °C, the flexural strength of (Ti,Zr,Nb)C medium-entropy ceramics containing 33.3 at% Zr and 40 at% Zr is 875 ± 43 and 843 ± 71 MPa, respectively. The relatively smooth grain boundaries observed at 1 000 °C changed to curved and serrated grain boundaries at 1 900 °C. The crack healing and crack tip blunting at high temperature may make a potential contribution to the clear increase in flexural strength.

Hf has about the same atomic radius as Zr, but there have been few reports on the densification of (Ti,Hf,Ta)C ceramics and their high-temperature mechanical properties up to now. In the present study, (Ti,Hf,Ta)C powders with low oxygen impurity are synthesized with carbothermal reduction method. The effects of the Hf content on sintering, microstructure and high-temperature strength of entropic ceramics in (Ti,Hf,Ta) C were investigated.

II. Experimental Procedure

(1) Sample preparation

The original powders were titanium oxide (TiO_2, 99.99 %, ~ 0.1 μm), hafnium oxide (HfO_2, 99.95 %, ~ 0.2 μm), tantalum pentoxide (Ta_2O_5, 99.9 %, ~ 1.5 μm), and graphite (99.9 % pure, ~ 2 μm). The original powders were mixed in a molar ratio of 2:2:1:19 (TiO_2: HfO_2: Ta_2O_5: graphite) according to the reaction equation shown in Table 1 to obtain equimolar-ratio ceramics. After ball mixing, the mixed slurry was vacuumed to remove ethanol. Subsequently, it was further dried in an oven at 60 °C to obtain raw mixed powders with the name THTOC. The obtained THTOC powder was heated up to 1 400 – 1 700 °C for 0 ~ 1.5 h under vacuum atmosphere to prepare medium-entropy carbide powder (named as THTC) by means of carbothermal reduction. In order to adjust the Hf element content, $(Ti_{0.4}Hf_{0.2}Ta_{0.4})C$ and $(Ti_{0.3}Hf_{0.4}Ta_{0.3})C$ ceramic powders were also prepared with the same method with the TiO_2:HfO_2:Ta_2O_5:C molar ratios of 2:1:1:16 and 6:8:3:63, and named THTC-2 and THTC-4, respectively, as shown in Table 1.

Table 1: Reaction equations for (Ti,Hf,Ta)C compositions with different Hf content.

Name	Reaction equations for different compositions
THTC	$2TiO_2 + 2HfO_2 + Ta_2O_5 + 19C \rightarrow 6(Ti_{1/3}Hf_{1/3}Ta_{1/3})C + 13CO\ (g)$
THTC-2	$2TiO_2 + HfO_2 + Ta_2O_5 + 16C \rightarrow 5(Ti_{0.4}Hf_{0.2}Ta_{0.4})C + 11CO\ (g)$
THTC-4	$6TiO_2 + 8HfO_2 + 3Ta_2O_5 + 63C \rightarrow 20(Ti_{0.3}Hf_{0.4}Ta_{0.3})C + 43CO\ (g)$

The obtained THTC powders were sieved through a 200-mesh screen, and then placed into a 30 mm × 37 mm graphite die lined with graphite paper. The THTC powders were sintered by means of hot pressing at 1 900 – 2 100 °C for 1 h at a heating rate of 10 K/min to obtain rectangular samples with the dimensions 30 mm × 37 mm × 5 mm (width × length × thickness). The furnace was heated under < 10 Pa vacuum to 1 650 °C, and the chamber was backfilled with high-purity argon (> 99.999 purity). A uniaxial pressure of 30 MPa was applied at 1 650 °C at a rate of 3 MPa/min. After soaking, the pressure was decreased to 2 kN at a rate of 5 kN/min, then the pressure-controlling program was turned off. The temperature was dropped at a rate of 15 K/min from soaking temperature to 1 700 °C and the sample was naturally cooled down to room temperature. The obtained THTC-2 and THTC-4 powders were also sintered at 2 100 °C, in order for us to investigate the effects of Hf element content on the densification and microstructure of (Ti,Hf,Ta)C ceramics. TaC powders and ceramics were also prepared with the same method as that applied for the THTC. The as-sintered samples were ground on both sides to remove the graphite foil and reaction layers. Densities were measured with the Archimedes method using distilled water as the immersing medium. Theoretical densities were calculated from the lattice parameters, which were determined by means of XRD refinement.

(2) Characterization of the structure and properties

X-ray diffraction (XRD, D8 ADVANCE, Bruker, Germany) was used to determine the phase compositions of the THTC powders and ceramics with Cu-Kα radiation. Jade 5.0 software was used to refine the XRD patterns and calculate the lattice parameters. An oxygen/nitrogen analyzer (TC-600C, Leco, USA) was used to measure the oxygen content in the THTC powders. The microstructure of the powders and ceramic specimens was characterized with an FESEM (Magellan 400L, FEI, USA) and SEM (TM3000, Hitachi, Japan). Rectangular bars measuring 30 mm × 2.5 mm × 2.0 mm (length × width × thickness) were cut from the sintered blocks by means of wire-cut electrical discharge machining. The bars were ground, polished to 0.5 μm finish using a diamond paste, and then the edges were chamfered. An ultra-high-temperature strength testing machine (AG-X Plus, Shimadzu, Japan) was used to measure the four-point flexural strength. The inner and outer spans were 10 mm and 20 mm, respectively. Different crosshead rates were set to 0.5 mm/min at 25 – 1 000 °C and 2 mm/min at 1 600 – 1 800 °C. At least three measurements were performed for each type of sample to calculate the average strength.

III. Results and Discussion

The XRD patterns of THTOC powders heated at 1 600 – 1 700 °C are shown in Fig. 1(a). It can be seen that at 1 600 °C without holding time (0 h), residual graphite and HfO_2 phases are still present in the reaction products. When they are heated at 1 600 – 1 700 °C and with a holding time extended to 1.5 h, they exhibit a biphasic composition. Based on comparison of the XRD patterns with the ICDD-PDF of HfC (No. 39 – 1491), TiC (No. 32 – 1383), TaC (No. 35 – 0801), Hf(Ti,Ta)C and Ti,Ta(Hf)C phases were identified in the THTC powders. The oxygen content of the THTC powders at 1 600 °C for 1.5 h and 1 700 °C for 1.5 h was 0.61 wt% and 0.42 wt%, respectively. Since the THTC powder has the lower oxygen content at 1 700 °C for 1.5 h, this was used as the original powder for the preparation of THTC ceramics.

In order to understand the carbothermal reaction processes and the formation reasons for the biphasic compositions in THTC powder, THTOC powders were also heated at 1 400 – 1 500 °C without holding time and their XRD patterns are shown in Fig. 1(b). At 1 400 °C, the XRD peaks of TiO_2 and Ta_2O_5 disappeared, and peaks of $TiTaO_4$ appeared. Meanwhile, there was a large amount of residual HfO_2, indicating that the reaction rate of the TiO_2-Ta_2O_5 binary system forming $TiTaO_4$ was higher than HfO_2-Ta_2O_5 and HfO_2-TiO_2. According to the TiO_2-Ta_2O_5 phase diagram proposed by Waring and Roth [26], $TiTa_2O_7$ solid solution can form in this binary system at a temperature of about 1 400 °C in air. In the present study, the presence of graphite in the mixed THTOC powders and the vacuum atmosphere could promote the formation of $TiTaO_4$ solid solution at 1 400 °C with holding time. With the increase of temperature up to 1 500 °C, the $TiTaO_4$ peaks disappeared, the graphite peak intensity decreased, and meanwhile Ti,Ta(Hf)C peak intensity increased, which indicated that most of $TiTaO_4$ was reduced to Ti,Ta(Hf)C by graphite. From 1 400 °C to 1 500 °C, the HfO_2 peaks intensity does not change much, and the XRD peak intensity of Hf(Ti,Ta)C was lower than that of Ti,Ta(Hf)C at 1 500 °C. From the XRD patterns, it can be concluded that $TiTaO_4$ performs carbothermal reduction reaction more preferentially, and also much faster than HfO_2. $TiTaO_4$ and its carbothermal reduction product Ti,Ta(Hf)C may coat or disperse around HfO_2 particles and therefore could inhibit the diffusion of HfO_2 particles and their grain growth. Liu *et al.* [27] synthesized ultra-fine HfC powders (particle size of 225 nm) based on a carbothermal reaction of HfO_2 with carbon black. The results showed that limiting the HfO_2 particle grain growth can decrease HfC powder grain size. When heated at 1 600 – 1 700 °C with a holding of 1.5 h, it shows a biphasic composition with Hf(Ti,Ta)C and Ti,Ta(Hf)C phases. Fig. 2 shows the back-scattered electron images of the synthesized THTC powder after heating at 1 700 °C for 1.5 h. The THTC powder is fine with the particle size of about 200 – 300 nm. The dark phase is Ti,Ta(Hf)C and the bright phase is Hf(Ti,Ta)C.

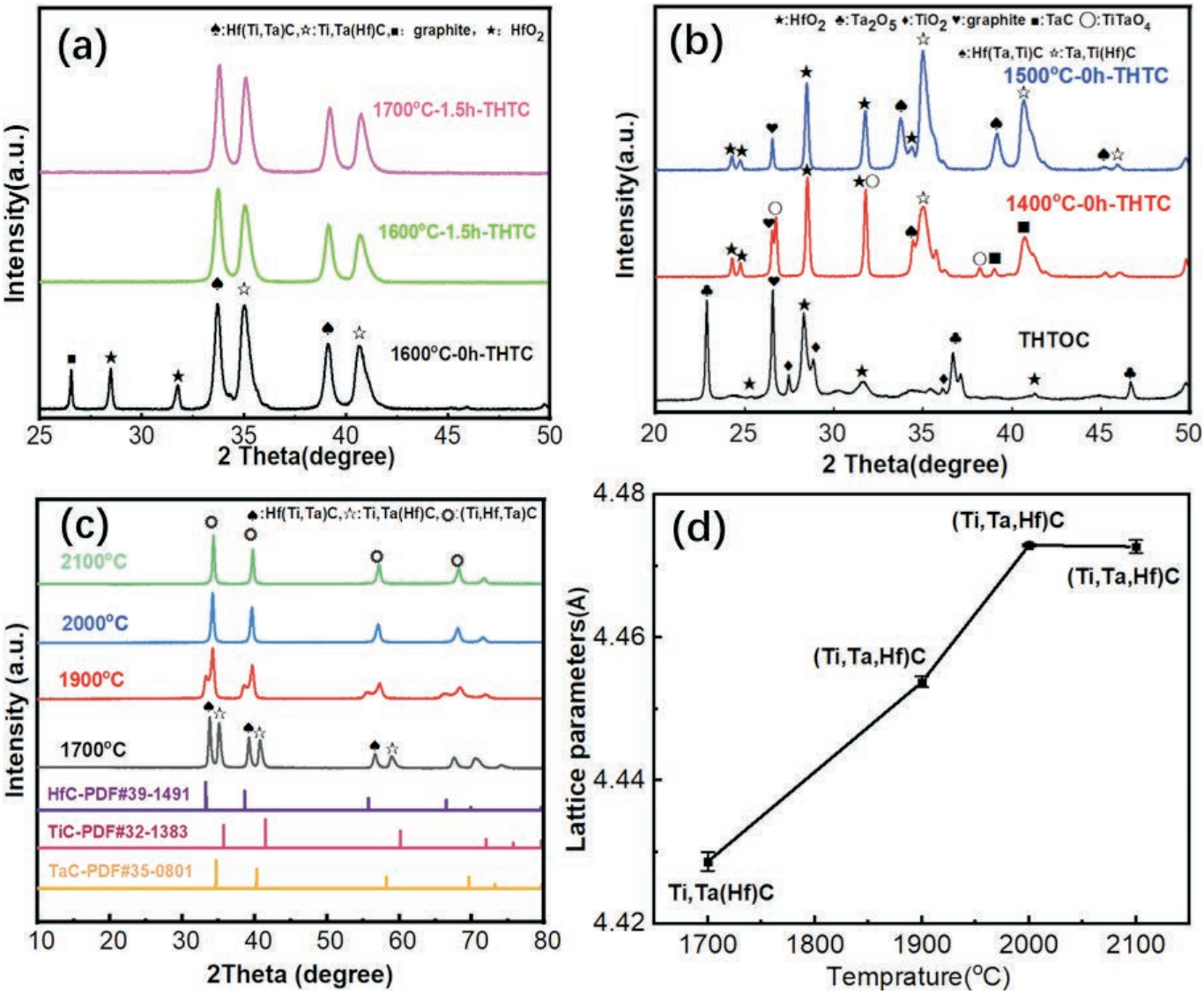

Fig. 1: XRD patterns of the THTC powders at 1 600 – 1 700 °C (a), the THTOC powder, and THTC powders at 1 400 – 1 500 °C (b), THTC powders (1 700 °C) and THTC ceramics sintered at 1 900 – 2100 °C (c), and the lattice parameters of Ti,Ta(Hf)C phase at 1 700 °C and (Ti,Ta,Hf)C in THTC ceramics sintered at 1 900 – 2 100 °C (d).

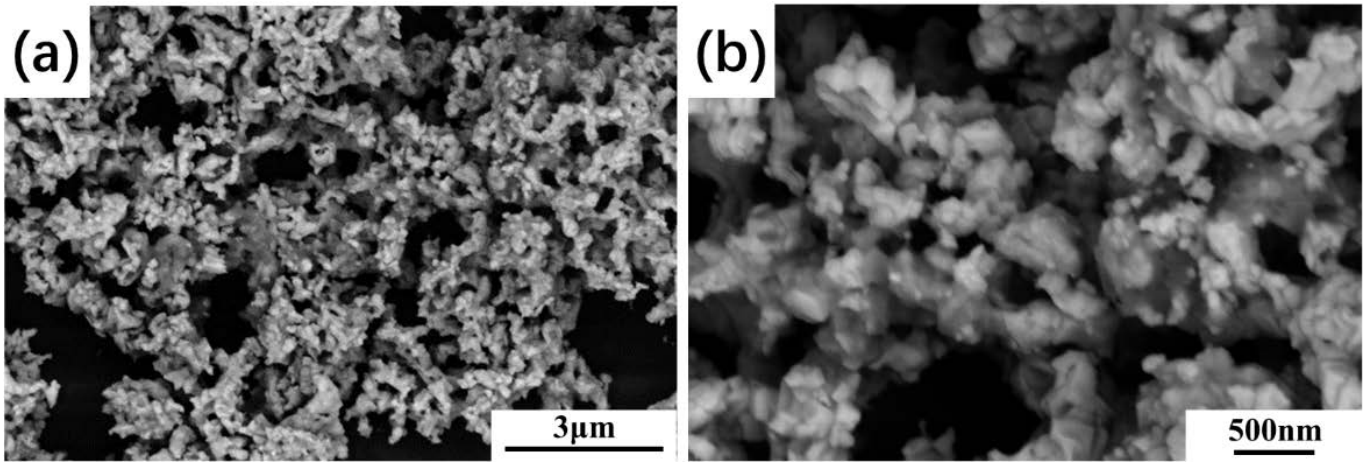

Fig. 2: SEM images at different magnifications for THTC powders synthesized at 1 700 °C for 1.5 h, (a) ×10 000, (b) ×30 000.

THTC powders were sintered at 1 900 – 2 100 °C with the hot-pressing method. Fig. 1(c) shows the XRD patterns of THTC ceramics sintered at different temperatures (1 900 °C, 2 000 °C, and 2 100 °C) for 1 h. The satellite peaks of Hf(Ti,Ta)C in THTC ceramics sintered at 1 900 °C (Fig. 1 c) could confirm that the (Ti,Hf,Ta)C solid solution was inhomogeneous. As the sintering temperature rose to 2 000 – 2 100 °C, the Hf(Ti,Ta)C peak disappeared, and single-phase (Ti,Hf,Ta)C solid solution with the composition of $(Ti_{1/3}Hf_{1/3}Ta_{1/3})C$ was finally formed. The lattice parameters of Ti,Ta(Hf)C in THTC powders at 1 700 °C and (Ti,Hf,Ta)C in THTC ceramics sintered at 1 900 – 2 100 °C are shown in Fig. 1(d). The lattice parameter of Ti,Ta(Hf)C phase and Hf(Ti,Ta)C phase in THTC powders at 1 700 °C is 4.4287 Å and 4.6057 Å, respectively. After sintering at 1 900 °C, the lattice parameter of (Ti,Hf,Ta)C is 4.4538 Å. It increased up to 4.4729 Å at 2 000 °C, which is due to the formation of the (Ti,Hf,Ta)C solid solution between Hf(Ti,Ta)C and Ti,Ta(Hf)C. The lattice parameters of (Ti,Hf,Ta)C at 2 100 °C (4.4716 Å) were about same as those at 2 000 °C, indicating that Hf(Ti,Ta)C and Ti,Ta(Hf)C nearly formed homogeneous solid solutions of (Ti,Hf,Ta)C at 2 100 °C.

Fig. 3 shows a comparison of the relative densities of THTC and single carbides (TiC[9], HfC[9] and TaC) sintered at different temperatures. The relative density of THTC ceramics sintered at 2 000 °C is only 78.5 %, which is much lower than that of corresponding monocarbide TiC[9], TaC, and HfC[9] (98.8 %, 91.7 %, and 88.6 %, respectively) sintered at 2 000 °C. At 2 100 °C the relative density of THTC (93.3 %) was higher than that of HfC (91.8 %), and lower than that of TaC (98.8 %). The melting points of TiC, TaC, and HfC were 3 027 °C, 3 880 °C, and 3 959 °C, respectively. HfC has the highest melting temperature, which indicates that it has the lowest atomic mobility at a specified temperature. Therefore, in the monocarbides, HfC was much harder to sinter dense than TiC and TaC. In order to investigate the effect of Hf element on the densification of (Ti,Hf,Ta)C ceramics, (Ti,Hf,Ta)C ceramics with different Hf content (20 at%, 33.3 at%, and 40 at%), corresponding to $(Ti_{0.4}Hf_{0.2}Ta_{0.4})C$, $(Ti_{1/3}Hf_{1/3}Ta_{1/3})C$ and $(Ti_{0.3}Hf_{0.4}Ta_{0.3})C$, were sintered at 2 100 °C. The theoretical density of THTC-2, THTC and THTC-4 was 10.59, 10.98 and 11.18 g/cm^3, respectively. The relative density of THTC-2, THTC, and THTC-4 sintered at 2 100 °C was 97.5 %, 93.3 %, and 92.7 %, respectively. With the increase of the Hf element content in (Ti,Hf,Ta)C ceramics, the relative density of the (Ti,Hf,Ta)C ceramics decreased. It can be concluded that Hf element inhibited the densification of (Ti,Hf,Ta)C ceramics owing to its very low atomic mobility.

Fig. 4 shows SEM images of the polished surfaces for TiC, HfC, TaC ceramics with high relative densities sintered at 2 000 – 2 200 °C, and THTC-2, THTC, THTC-4 ceramics sintered at 2 100 °C. It can be seen that compared with TiC, HfC, and TaC, THTC and THTC-4 exhibit a much finer microstructure. The average grain sizes of TiC, HfC, TaC, THTC-2, THTC, and THTC-4 are 13.5 ± 4.8 μm, 14.0 ± 4.9 μm, 5.7 ± 1.7 μm, 5.35 ± 1.8 μm, 0.92 ± 0.4 μm, and 1.1 ± 0.3 μm, respectively. For monocarbide ceramics, the grain boundary migration speed is higher than the pore elimination speed at densification temperature. Therefore, the rapid grain coarsening caused the large grain size and high content of closed pores entrapped in the grains. For (Ti,Hf,Ta)C ceramics, it can be seen that the Hf element obviously inhibited the grain size of (Ti,Hf,Ta)C ceramics. The higher the content of Hf element, the smaller the ceramic grain size. For $(Ti_{1/3}Hf_{1/3}Ta_{1/3})C$ and $(Ti_{0.3}Hf_{0.4}Ta_{0.3})C$ ceramics, the pores were primarily located at the grain boundaries and the triple points. Based on the above results, it can be concluded that the formation of equimolar ratio $(Ti_{1/3}Hf_{1/3}Ta_{1/3})C$ medium-entropy ceramics can significantly inhibit grain growth during sintering.

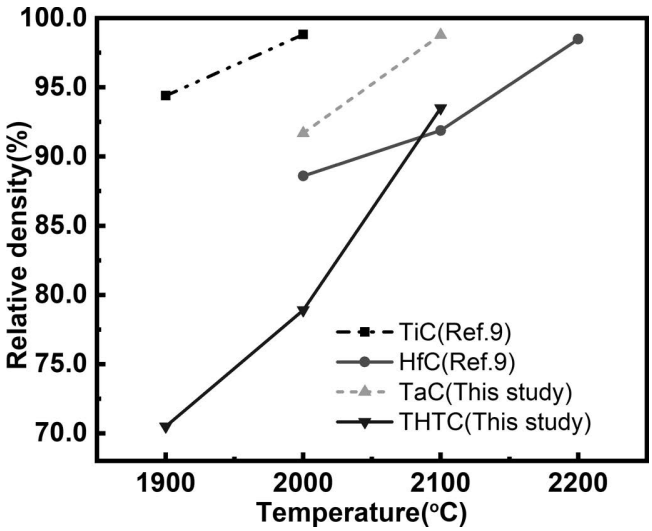

Fig. 3: Relative densities of TiC[9], HfC[9], TaC and THTC ceramics at different sintering temperatures.

Fig. 5(a) shows the room temperature and high-temperature (1 000 – 1 800 °C) flexural strength of THTC ceramics sintered at 2 100 °C, TiC sintered at 2 000 °C, TaC sintered at 2 100 °C, and HfC sintered at 2 200 °C. The flexural strength of THTC at room temperature (335 ± 34 MPa) is inferior to HfC (372 ± 75 MPa) [9], TiC (427 ± 99 MPa) [9], and TaC (431 ± 104 MPa). The present of a higher content of pores in THTC than monocarbide is responsible for the lower flexural strength at room temperature. The flexural strength of THTC (510 ± 59 MPa) at 1 000 °C increased compared with room temperature. In contrast, the flexural strengths of monocarbide ceramics TiC, TaC, HfC at 1 000 °C obviously decreased to 359 ± 124 MPa[9], 389 ± 55 MPa, and 261 ± 32 MPa[9], respectively. As the temperature increases further, the flexural strength of THTC reached 639 ± 38 MPa at 1 600 °C and an ultra-high strength of 697 ± 26 MPa at 1 800 °C. The grain size of THTC is much smaller than that of the corresponding monocarbide ceramics, which also explains the higher high-temperature flexural strength. Meanwhile, the inter-diffusion in the formation of a medium-entropy solid solution also increased the grain boundary strength of THTC. In addition, the pores were rounded off at high temperature, which blunted the crack tips at the specimen surface and decreased the critical flaw size. The evolution of pores and its

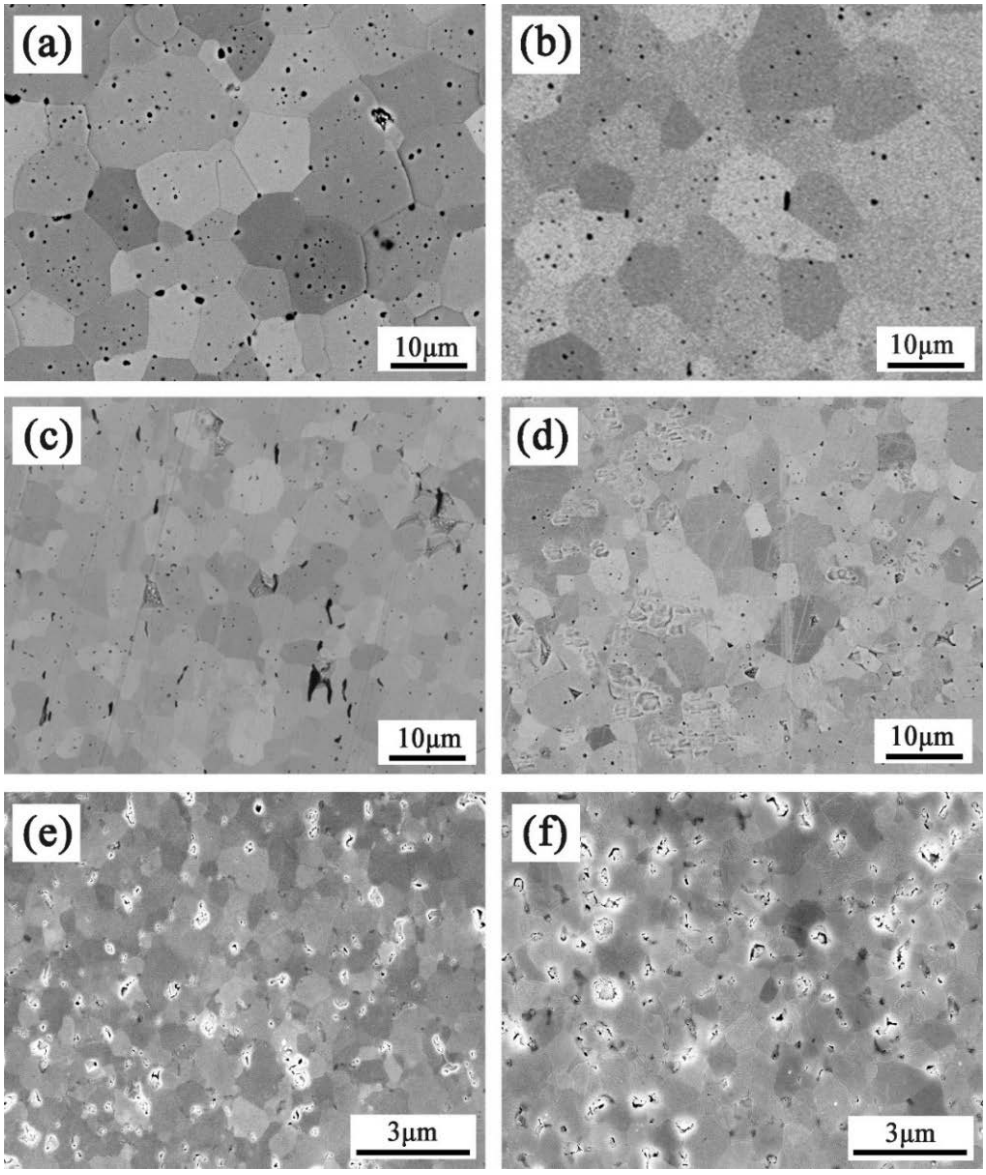

Fig. 4: SEM images of the polished surfaces of TiC sintered at 2 000 °C (a), HfC sintered at 2 200 °C (b), TaC sintered at 2 100 °C (c), and THTC-2 (d), THTC (e), THTC-4 (f) ceramics sintered at 2 100 °C.

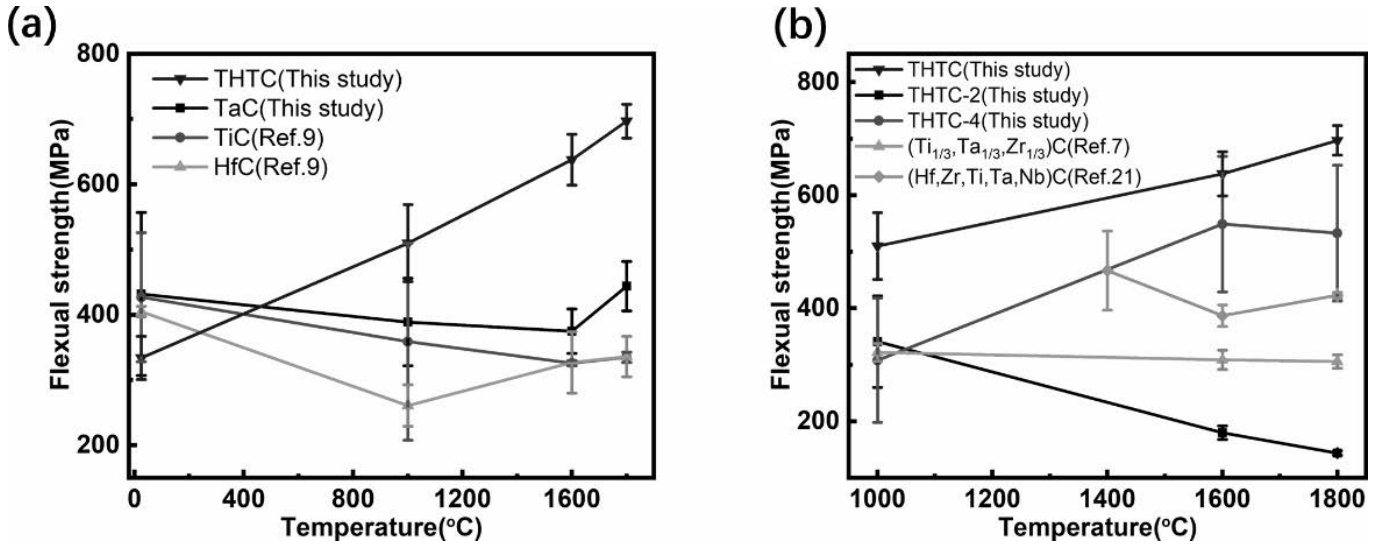

Fig. 5: Flexural strength as a function of temperature for THTC, and monocarbide (TiC[9], HfC[9], TaC) ceramics(a), and (Ti,Hf,Ta)C compared with ($Ti_{1/3}$,$Ta_{1/3}$,$Zr_{1/3}$)C[7], (Hf,Zr,Ti,Ta,Nb)C[21] ceramics (b).

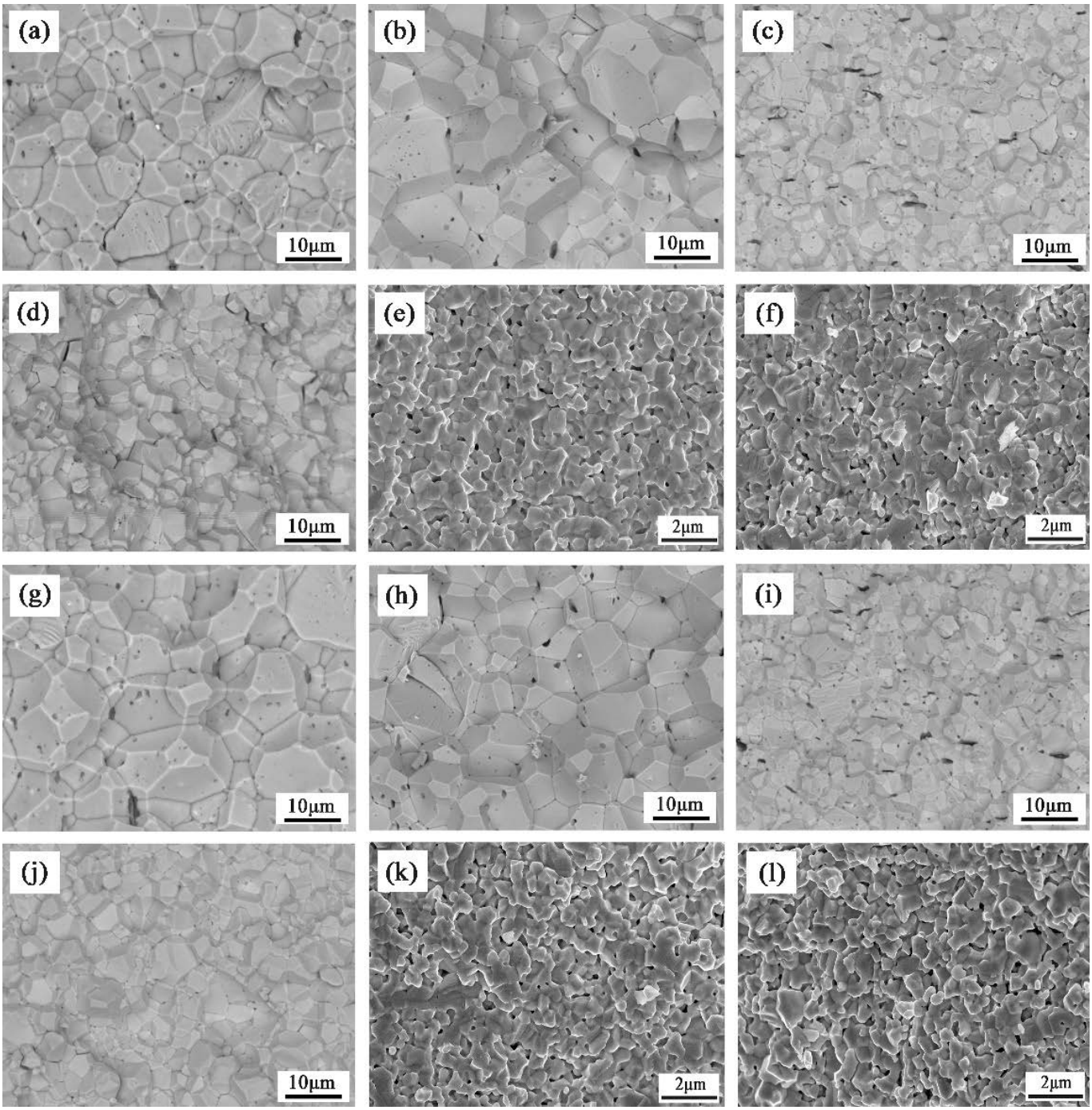

Fig. 6: Fracture surfaces of TiC (a, g), HfC (b, h), TaC (c, i), THTC-2 (d, j), THTC (e, k), and THTC-4 (f, l) ceramics at different test temperatures, (a-f) at 25 °C, and (g-l) at 1 800 °C.

effect on fracture origin at high temperature needs further investigation. Fig. 5(b) shows the flexural strength of THTC-2, THTC, THTC-4, $(Ti_{1/3}Ta_{1/3}Zr_{1/3})C$[7] ceramics at 1 000 – 1 800 °C and (Hf,Zr,Ti,Ta,Nb)C [21] ceramics at 1 400 – 1 800 °C. The flexural strength of THTC at 1 000 – 1 800 °C (510 – 697 MPa) was clearly higher than that of THTC-2 (144 – 341 MPa), and THTC-4 (308 – 579 MPa). The high-temperature flexural strength of THTC ceramics at 1 000 – 1 800 °C is much higher than that of the $(Ti_{1/3}Ta_{1/3}Zr_{1/3})C$ ceramics (294 – 338 MPa) at 1 000 – 1 800 °C reported by Demirskyi *et al.* [7] and (Hf,Zr,Ti,Ta,Nb)C high-entropy ceramics (397 – 428 MPa) reported by Feng *et al.* [21] at 1 400 – 1 800 °C. The high strength of THTC was mainly attributed to the moderate Hf content, which inhibited the phenomenon of fast grain growth in the sintered THTC.

The fracture surfaces of THTC were compared with those of monocarbide, THTC-2 and THTC-4 (shown in Fig. 6). As can be seen, the fracture modes of THTC and THTC-4 were very different from THTC-2 and monocarbide. Although the pore content of THTC and THTC-4 is 6.7 % and 7.3 %, respectively, the grain boundary of THTC and THTC-4 was significantly enhanced by the solid solution with moderate Hf content. THTC and THTC-4 exhibited a mixture of transgranular and intergranular fracture mode at 25 °C. As the temperature in-

creased to 1 800 °C, the transgranular cleavage (as shown in Fig. 6k) is still found. Conversely, THTC-2 and monocarbide showed a mixture of transgranular and intergranular fracture mode at 25 °C, and completely intergranular mode at 1 800 °C, which explained their much weaker grain boundary strength than THTC and THTC-4 ceramics.

IV. Conclusions

In summary, the medium-entropy (Ti,Hf,Ta)C-based powders with biphasic composition of Hf(Ti,Ta)C and Ti,Ta(Hf)C were prepared by means of carbothermal reduction of TiO_2, Ta_2O_5, HfO_2 with graphite in vacuum at 1 700 °C. TiO_2 and Ta_2O_5 formed $TiTaO_4$ solid solution at 1 400 °C, which performed carbothermal reduction reaction more preferentially, and also much faster than HfO_2. $TiTaO_4$ and Ti,Ta(Hf)C had the effect of inhibiting HfO_2 grain growth. The resulting (Ti,Hf,Ta)C-based powders had a fine particle size of 200 – 300 nm and low oxygen content of 0.42 wt%. After sintering at 2 100 °C for 1 h, single-phase (Ti,Hf,Ta)C ceramics were obtained. The Hf element significantly inhibited the densification and grain growth of (Ti,Hf,Ta)C medium-entropy ceramics due to its lattice distortion and sluggish diffusion effects. Compared with the monocarbide ceramics (TiC, HfC, TaC), equimolar ratio (Ti,Hf,Ta)C corresponding to (Ti,Hf,Ta)C has a finer grain size and higher high-temperature strength. (Ti,Hf,Ta)C had ultra-high strength at 1 600 °C (639 ± 38 MPa) and 1 800 °C (697 ± 26 MPa). The ultra-high strength of (Ti,Hf,Ta)C medium-entropy ceramics is the result of the collaborative optimization of their superfine microstructure (grain size of 0.92 ± 0.4 μm) and strong grain boundary strength.

Acknowledgements

Financial support from the National Natural Science Foundation of China (No. 52172076) and from the State Key Laboratory of High-Performance Ceramics and Superfine Microstructure is greatly appreciated.

References

1 Castle, E.G., Csanadi, T., Grasso, S., Dusza, J., Reece, M.: Processing and properties of high-entropy ultra-high temperature carbides, *Sci. Rep.,* **8,** 8 – 20, (2018).

2 Failla, S., Galizia, P., Fu, S., Grasso, S., Sciti, D.: Formation of high entropy metal diborides using arc-melting and combinatorial approach to study quinary and quaternary solid solutions, *J. Eur. Ceram. Soc.,* **40,** 588 – 593, (2020).

3 Xiang, H., Xing, Y., Dai, F.Z., Wang, H.J., Su, L., Miao, L., Zhang, G.J., Wang, Y.G., Qi, X.W., Yao, L., Wang, H.L., Zhao, B., Li, J.Q., Zhou, Y.C.: High-entropy ceramics: Present status, challenges, and a look forward, *J. Adv. Ceram.,* **10,** 385 – 441, (2021).

4 Fahrenholtz, W.G., Hilmas, G.E.: Ultra-high temperature ceramics: materials for extreme environments, *Scripta Mater.,* **129,** 94 – 99, (2017).

5 Nisar, A., Zhang, C., Boesl, B., Agarwal, A.: A perspective on challenges and opportunities in developing high entropy-ultra high temperature ceramics, *Ceram. Int.,* **46,** 25845a – 25853a, (2020).

6 Liu, J., Yang, Q.Q., Zou, J., Wang, W.M., Wang, X.G., Fu, Z.Y.: Strong high-entropy diboride ceramics with oxide impurities at 1800 °C, *Sci. China Mater.,* **84,** 1 – 10, (2023).

7 Demirskyi, D., Nishimurab, T., Suzuki, T.S., Sakka, Y., Vasylkivb, O., Yoshimi, K.: High-temperature toughening in ternary medium entropy $(Ta_{1/3}Ti_{1/3}Zr_{1/3})C$ carbide consolidated using spark plasma sintering, *J. Am. Ceram. Soc.,* **8,** 1262 – 1270, (2020).

8 Yang, Q.Q., Wang, X.G., Wu, P., Wang, X.F., Zhang, C., Zhang, G.J., Jiang, D.Y.: Ultra-high strength medium entropy (Ti,Zr,Ta)C ceramics at 1800 °C sintered from medium-entropy powders with a core-shell structure, *J. Am. Ceram. Soc.,* **105,** 823 – 829, (2022).

9 Wang, X.F., Wang, X.G., Yang, Q.Q., Dong, H.L., Zhang, C., Zhang, G.J., Jiang, D.Y.: High-strength medium-entropy (Ti,Zr,Hf)C ceramics up to 1800 °C, *J. Am. Ceram. Soc.,* **104,** 2436 – 2441, (2021).

10 Wang, H.X., Liu, Q.M., Wang, Y.G.: Research Progress of High-entropy Transition Metal Carbide Ceramics, *J. Inorg. Mater.,* **36,** 355 – 364, (2021).

11 Zhang, G.J., Wang, Y.J.: Non-order is the New Order: High-entropy Ceramics, *J. Inorg. Mater.,* **36,** 337 – 338, (2021).

12 Simonenko, E.P., Sevast'yanov, D.V., Simonenko, N.P., Sevast'yanov, V.G., Kuznetsova, N.T.: Promising ultra-high-temperature ceramic materials for aerospace applications, *Russ. J. Inorg. Chem.,* **58,** 1669 – 1693, (2013).

13 Chen, T.K., Shun, T.T., Yeh, J.W., Wong, M.S.: Nanostructured nitride films of multi-element high-entropy alloys by reactive DC sputtering, *Surf. Coat. Technol.,* **188 – 189,** 193 – 200, (2004).

14 Hsu, C.Y., Yeh, J.W., Chen, S.K., Shun, T.T.: Wear resistance and high temperature compression strength of FCC CuCoNi-$CrAl_{0.5}Fe$ alloy with boron addition, *Metall. Mater. Trans.,* **35A,** 1465 – 1469, (2004).

15 Qin, Y., Liu, J.X., Liang, Y.C., Zhang, G.J.: Equiatomic 9-cation high-entropy carbide ceramics of the IVB, VB, and VIB groups and thermodynamic analysis of the sintering process, *J. Adv. Ceram.,* **11,** 1082 – 1092, (2022).

16 Zhang, Y., Sun, S.K., Guo, W.M., Xu, L., Zhang, W., Lin, H.T.: Optimal preparation of high-entropy boride-silicon carbide ceramics, *J. Adv. Ceram.,* **10,** 173 – 180, (2021).

17 Xu, L., Guo, W.M., Zou, J., Zhou, Y.Z., Liang, H.Y., Qiu, S.H., Lin, H.T., Fu, Z.: Low-temperature densification of high entropy diboride based composites with fine grains and excellent mechanical properties, *Compos. Part B-Eng.,* **247,** 110331, (2022).

18 Qin, M.D., Yan, Q.Z., Liu, Y., Luo, J.: A new class of high-entropy M_3B_4 borides, *J. Adv. Ceram.,* **10,** 166 – 172, (2021).

19 Demirskyi, D., Suzuki, T.S., Yoshimi, K., Vasylkiv, O.: Synthesis and high-temperature properties of medium-entropy (Ti,Ta,Zr,Nb)C using the spark plasma consolidation of carbide powders, *Open Ceramics.,* **2,** 100015, (2020).

20 Sun, Y.N., Ye, L., Zhao, W.Y., Chen, F.H., Qiu, W.F., Han, W.J., Liu, W., Zhao, T.: Synthesis of High-entropy Carbide Nano Powders via Liquid Polymer Precursor Route, *J. Inorg. Mater.* **36,** 393 – 398, (2021).

21 Feng, L., Chen, W.T., Fahrenholtz, W.G., Hilmas, G.E.: Strength of single-phase high-entropy carbide ceramics up to 2300 °C, *J. Am. Ceram. Soc.,* **104,** 419 – 427, (2021).

22 Li, F., Lu, Y., Wang, X.G., Bao, W.C., Liu, J.X., Xu, F.F., Zhang, G.J.: Liquid precursor-derived high-entropy carbide nanopowders, *Ceram. Int.,* **45,** 22437 – 22441, (2019).

23 Guo, X.J., Bao, W.C., Liu, J.X., Wang, X.G., Zhang, G.J., Xu, F.F.: Study on the Solid Solution Structures of High-entropy Ceramics by Transmission Electron Microscopy, *J. Inorg. Mater.,* **36,** 365 – 374, (2021).

24 Zhang, W., Chen, L., Xu, C.G., Lv, X.M., Wang, Y.J., Ouyang, J.H., Zhou, Y.: Grain growth kinetics and densification mechanism of (TiZrHfVNbTa)C high-entropy ceramic under

pressureless sintering, *J. Mater. Sci. Technol.,* **110,** 57 – 64, (2022).

[25] Yang, Q.Q., Wang, X.G., Bao, W.C., Wu, P., Wang, X.F., Guo, X.J., Zhang, C., Zhang, G.J., Jiang, D.Y.: Influence of equiatomic Zr/(Ti,Nb) substitution on microstructure and ultra-high strength of (Ti,Zr,Nb)C medium-entropy ceramics at 1900 °C, *J. Adv. Ceram.,* **11,** 1457 – 1465, (2022).

[26] Waring, J.L., Roth, R.S.: Effect of oxide additions on the polymorphism of tantalum pentoxide system Ta_2O_5-TiO_2, *J. Research of the National Bureau of Standards-A. Phys. Chem.,* **2,** 175 – 186, (1968).

[27] Liu, J.X., Kan, Y.M., Zhang, G.J.: Synthesis of ultra-fine hafnium carbide powder and its pressureless sintering, *J. Am. Ceram. Soc.,* **93,** 980 – 986, (2010).